

Frequency response of optical beam deflection by ultrasound in water

James N. Caron^{1,2,*} and Greg P. DiComo¹

¹Research Support Instruments, 4325-B Forbes Boulevard, Lanham, Maryland 20706, USA

²Quartet, 205 Indian Spring Drive, Silver Spring, Maryland 20901, USA

*Corresponding author: Caron@RSImd.com

Received 27 June 2014; revised 19 September 2014; accepted 23 September 2014;
posted 7 October 2014 (Doc. ID 214881); published 5 November 2014

Acoustic waveforms create fluctuations in the index of refraction of the medium. An optical beam passing through the disturbance will be deflected or displaced from the original path. The acoustic wave can be detected by sending a laser through the disturbance and sensing the path changes of the beam with a position-sensitive photodetector. This paper presents a model of this interaction in water to predict the sensitivity and frequency response. The model demonstrates that the frequency response of the system is broadband, allowing detection from a few hundred hertz to 20 MHz. This technique has potential use for underwater acoustic sensing and ultrasonic inspection of materials. © 2014 Optical Society of America

OCIS codes: (230.1040) Acousto-optical devices; (280.3420) Laser sensors; (280.5475) Pressure measurement.

<http://dx.doi.org/10.1364/AO.53.007677>

1. Introduction

An optical beam is diverted from the original path as it passes through an acoustic field, as a result of variations in the medium's index of refraction. Depending on the size of the beam and the acoustic waveform, the interaction can take the form of a deflection or a displacement [1]. This provides a method to sense ultrasound remotely without affecting the traveling wave. In a gas medium, this technique is designated gas-coupled laser acoustic detection (GCLAD) [2] and has been used to sense audio-frequency waves and ultrasound waves [3]. The method has proven to be a relatively simple and effective method for sensing ultrasound that has been transmitted from materials, useful for material characterization and nondestructive evaluation [4].

The purpose of this paper is to further investigate the use of optical beam deflection where water serves as the medium. Several studies have demonstrated

the use of optical beam deflection for sensing ultrasound waves in water. For example, Diaci [5] developed a transfer function for detection of cylindrical waves using optical beam deflection and provided supporting empirical evidence. Matsuoka *et al.* [6] used this method to measure ultrasonic velocities in different liquids. The technique was used by Choi in 2000 to measure acoustic nonlinearity parameters and ultrasonic absorption in various liquids [7]. In 2006, Yamaguchi and Choi compared theoretical calculations and the empirical responses of a hydrophone [8]. Petkovšek and Možina in 2005 [9] and Gregorčič and Možina in 2007 [10] used optical beam deflection to sense shock waves created by laser-induced plasmas in water. In 2013, Caron and Kunapareddy measured the directivity of a 1 MHz piezoelectric transducer [11]. In this paper, the frequency response of optical beam deflection in water is determined where the acoustic source is a piston radiator.

Previous research with GCLAD has shown the utility of the technique for sensing flaws in composite materials [4]. A general rule of thumb states that the smallest detectable flaw needs to be larger than half

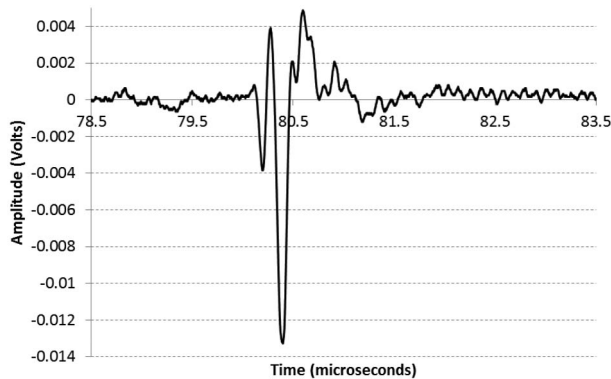


Fig. 1. This waveform, averaged over 16 shots, was generated with a 10 MHz transducer and sensed using the GCLAD system with water as the medium. The lower attenuation in water allows optical beam deflection to capture higher frequencies at greater distances. The distance from the transducer to the laser beam was 11.0 cm.

the wavelength of the ultrasound [12]. As with all air-coupled techniques, GCLAD is limited to frequencies of a few megahertz and below as a result of exponential attenuation in air [13]. To obtain higher frequencies with essentially the same instrumentation, the interrogation can take place in water, where attenuation is significantly less. Figure 1 shows a waveform produced by a 10 MHz transducer and captured by our system after propagating 11.0 cm in water. At this distance in air, the waveform would have been attenuated beyond the detection limit of the technique.

The term “optical beam deflection” has been used to describe the change in the path of an optical beam when the medium is altered by an acoustic waveform. To differentiate the technique from Bragg or Raman–Nath diffraction, the width of the beam is assumed to be smaller than the acoustic wavefront. In many papers [14–16], optical beam deflection has also been used to describe the situation where the beam is reflected off a surface that is modulated by an acoustic wave. In addition, in a recent paper [1], we demonstrated empirically that a displacement of the beam can be sensed in addition to deflection. As such, the scope of this paper is limited to the case where deflection has the form of an angular change in the beam path that is produced by an acoustic modulation in the medium.

2. Model Derivation

The acoustic source is modeled as a piston radiator that generates a waveform into the liquid medium, representing recent experimental research where a transducer generated an ultrasound wave into a tank of water [11]. As shown in Fig. 2, a laser beam is directed parallel to the source surface, but is offset by a distance such that the laser only interacts with the far-field propagation of the waveform. Following the optoacoustic interaction, positional changes in the optical beam are sensed by a bi-cell position-sensitive photodetector.

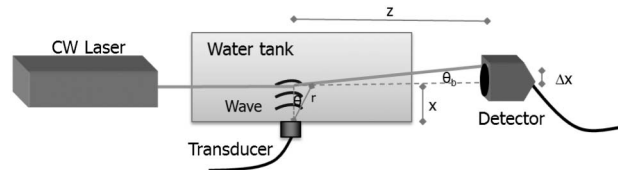


Fig. 2. Arrangement for sensing the deflection of a laser as a result of interaction with ultrasound in water. The acoustic wave travels a distance x before interacting with the laser beam. After interaction, the beam is deflected at angle θ_b until it is received by the photodetector.

This interaction produces both a displacement of the beam and a deflection, producing a signal that is a combination of both. The optical layout determines which component dominates the signal. If a convex lens is put in the path such that the beam is slightly out of focus at the detector, then the displacement component will dominate. If there is no lens, and the optical lever arm is sufficiently long, then the deflection will dominate the signal [1].

A. Acoustic Propagation

The ultrasound source is represented by the pressure distribution from a piston embedded in an infinite baffle [17]. The acoustic pressure produced in the far field by the piston is

$$p_f(r, \theta, t) = p_o \frac{e^{i(kr - \omega t)}}{r} \frac{2J_1(ak \sin \theta)}{ak \sin \theta}, \quad (1)$$

where r and θ are, respectively, the distance and the angle with respect to the center of the transducer, p_o is the original pressure amplitude, a is the radius of the piston, ω is the frequency of the modulation, and k is the wavenumber [18]. Since the calculation will be performed in Cartesian space, the cylindrical coordinates are related by $r = \sqrt{x^2 + z^2}$ and $\sin \theta = z/r$.

As the acoustic wave propagates, it decays according to the relationship

$$p(r, \theta, t) = p_f e^{-\alpha' \nu^2 r}, \quad (2)$$

where ν is the acoustic frequency [10,11] and α' is a frequency-independent attenuation coefficient in freshwater given by

$$\alpha' = \frac{4.34(2\pi)^2}{\rho_F c_F^3} \left(\frac{4\mu_F}{3} + \mu'_F \right), \quad (3)$$

where ρ_F is the freshwater density, c_F is the speed of sound in water, μ_F is the dynamic coefficient of shear viscosity, and μ'_F is the dynamic coefficient of bulk viscosity [18]. For freshwater, we have the values $\rho_F = 1000 \text{ kg/m}^3$, $c_F = 1461 \text{ m/s}$ at a temperature of 14°C , $\mu_F = 1.2 \times 10^{-3} \text{ Ns/m}^2$, and $\mu'_F = 3.3 \times 10^{-3} \text{ Ns/m}^2$. From Eqs. (2) and (3), we can compute the ratio of pressure at a specific distance to the original pressure, with some representative values

Table 1. Loss of Signal Amplitude due to Attenuation in Water Expressed as a Ratio of Pressure at a Specific Distance over the Original Pressure

Loss at	1 mm	1 cm	10 cm	1 m
1 kHz	1	1	1	1
10 kHz	1	1	1	0.999997
100 kHz	1	0.999997	0.999969	0.999690
1 MHz	0.999969	0.999690	0.996905	0.969482
10 MHz	0.996905	0.969482	0.733492	0.045077

shown in Table 1. The attenuation is generally inconsequential for frequencies of 1 MHz or below.

The propagation model takes the form

$$p(r, \theta, t) = p_o T e^{-\alpha v^2 r} \frac{e^{i(kr - \omega t)}}{r} \frac{2J_1(ak \sin \theta)}{ak \sin \theta}. \quad (4)$$

Pressure distributions for specific frequencies at a distance of $x = 10$ cm from the source are shown in Fig. 3. The graph demonstrates the decrease in amplitude resulting from attenuation and a sharp narrowing of the central peak.

B. Index of Refraction in Water

The relationship between pressure change and index of refraction variation in water must be determined. The International Association for the Properties of Water and Steam (IAPWS) presented a formulation that relates the refractive index of water as a function of wavelength, temperature, and pressure [19]. The relationship can be restated as

$$n = \sqrt{\frac{1 + 2\bar{\rho}A}{1 - \bar{\rho}A}}, \quad (5)$$

where $\bar{\rho}$ is the dimensionless density expressed as a ratio of the density of the medium and 1000 kg/m^3 . The coefficient A is a function of density, temperature, and optical wavelength, and can be expressed as

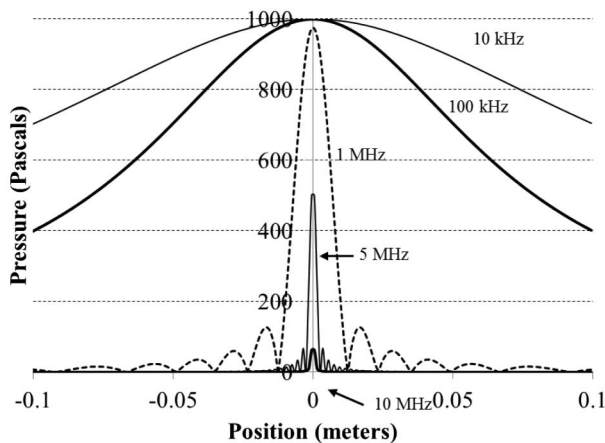


Fig. 3. Pressure distribution in water created by a piston source with a radius of 7.5 mm at a distance of $x = 10$ cm. The decrease in amplitude of the central peak for the higher frequency is the result of attenuation.

$$A = a_0 + a_1\bar{\rho} + a_2\bar{T} + a_3\bar{\lambda}^2\bar{T} + \frac{a_4}{\bar{\lambda}^2} + \frac{a_5}{\bar{\lambda}^2 - \bar{\lambda}_{UV}^2} + \frac{a_6}{\bar{\lambda}^2 - \bar{\lambda}_R^2} + a_7\bar{\rho}^2, \quad (6)$$

where \bar{T}_k and $\bar{\lambda}$ are the dimensionless temperature and wavelength, respectively. The coefficients are given in reference [19] and are reproduced in Table 2 alongside the derived quantities used in this derivation.

According to Hooke's law, a change in pressure Δp is approximately proportional to a change in density, or

$$\Delta p = \frac{B_w}{\rho_A} \Delta \rho, \quad (7)$$

where B_w is the bulk modulus of elasticity and ρ_A is the ambient density [18]. The approximation results from a slight time lag between the change in density and the change in pressure.

Equation (7) is used to represent the dimensionless density as a function of change in ambient pressure:

$$\bar{\rho} = \frac{\rho_A + \rho_A \Delta p / B_w}{\rho_A} = 1 + \frac{p(r, \theta, t)}{B_w}, \quad (8)$$

C. Relationship between Pressure and Index of Refraction

By defining a dimensionless pressure

$$\bar{p} = \bar{\rho} - 1, \quad (9)$$

Eq. (5) can be restated as

$$n = \sqrt{\frac{1 + 2(1 + \bar{p})A}{1 - (1 + \bar{p})A}}. \quad (10)$$

We wish to express this relationship in a form that will simplify later calculations. With constant temperature and laser wavelength, Eq. (6) can be restated as

$$A \equiv a_1\bar{\rho} + a_7\bar{\rho}^2 + a_8(\bar{T}, \bar{\lambda}) \equiv a_9 + a_{10}\bar{p} + a_7\bar{p}^2, \quad (11)$$

Table 2. Table of Constants and Derived Quantities

$a_0 = 0.244257733$	$a_1 = 9.74634476 \times 10^{-3}$
$a_2 = -3.73234996 \times 10^{-3}$	$a_3 = 2.65666426 \times 10^{-4}$
$a_4 = 2.45733798 \times 10^{-3}$	$a_5 = 2.45934259 \times 10^{-3}$
$a_6 = 0.900704920$	$a_7 = -1.66626219 \times 10^{-2}$
$\lambda_{UV} = 0.229202$	$\lambda_{IR} = 5.432937$
$a_8 \equiv a_0 + a_2\bar{T} + a_3\bar{\lambda}^2\bar{T} + \frac{a_4}{\bar{\lambda}^2} + \frac{a_5}{\bar{\lambda}^2 - \lambda_{UV}^2} + \frac{a_6}{\bar{\lambda}^2 - \lambda_{IR}^2}$	
$a_9 \equiv a_1 + a_8 + a_7$	$a_{10} \equiv a_1 + 2a_7$
$a_{11} \equiv a_9 + a_{10}$	$a_{12} \equiv a_7 + a_{10}$
$a_{14} \equiv 1 + 2a_9$	$a_{15} \equiv 1 - a_9$

producing

$$n(\bar{p}) = \sqrt{\frac{1 + 2(a_9 + a_{11}\bar{p} + a_{12}\bar{p}^2 + a_7\bar{p}^3)}{1 - (a_9 + a_{11}\bar{p} + a_{12}\bar{p}^2 + a_7\bar{p}^3)}}. \quad (12)$$

If no acoustic fluctuations are present, then Eq. (10) reduces to

$$n = \sqrt{\frac{1 + 2a_9}{1 - a_9}}. \quad (13)$$

For additional simplification, we define

$$\chi(\bar{p}) \equiv a_{11}\bar{p} + a_{12}\bar{p}^2 + a_7\bar{p}^3 \quad (14)$$

to produce

$$n(\bar{p}) = \sqrt{\frac{a_{14} + 2\chi(\bar{p})}{a_{15} - \chi(\bar{p})}}. \quad (15)$$

D. Optical Beam Deflection

The path of a light ray traveling along \hat{z} axis through a medium with a dynamic index of refraction $n(r, \phi, z)$ can be described by

$$\frac{d}{ds} \left(n(r, \phi, z) \frac{dr(r, \phi, z)}{ds} \right) = \nabla n(r, \phi, z), \quad (16)$$

where $r(r, \phi, z)$ is the ray trajectory and s is the scalar path length [20]. When the index of refraction fluctuations are primarily radial, Eq. (16) can be simplified to read as [21]

$$\frac{\partial^2 r(z)}{\partial z^2} = \frac{1}{n(r)} \frac{\partial n(r)}{\partial r}. \quad (17)$$

An additional simplification can be applied by assuming that the fluctuation is an acoustic wave traveling primarily along \hat{x} axis. Equation (17) can be restated as

$$\frac{\partial^2 x(z)}{\partial z^2} = \frac{1}{n(x, z)} \frac{\partial n(x, z)}{\partial x}. \quad (18)$$

The resulting beam deflection θ_b is assumed to be small such that

$$\theta_b = \tan^{-1} \left(\frac{dx}{dz} \right) \approx \frac{dx}{dz}, \quad (19)$$

producing

$$\frac{\partial \theta_b}{\partial z} \approx \frac{1}{n(x, z)} \frac{\partial n(x, z)}{\partial x}. \quad (20)$$

Integration with respect to z results in the relationship between the index of refraction and the optical beam deflection:

$$\theta_b \approx \int \frac{1}{n(x, z)} \frac{\partial n(x, z)}{\partial x} dz. \quad (21)$$

The derivative in Eq. (21) can be handled as the product of the partial derivatives,

$$\frac{\partial n(x, z)}{\partial x} = \frac{\partial n(x, z)}{\partial \chi} \frac{\partial \chi}{\partial \bar{p}} \frac{d\bar{p}}{dx}. \quad (22)$$

From Eq. (15), we can deduce

$$\frac{1}{n(x, z)} \frac{\partial n(x, z)}{\partial \chi} = \frac{a_{15} + a_{14}/2}{a_{14}a_{15} + \chi(2a_{15} - a_{14}) - 2\chi^2}. \quad (23)$$

The derivative of Eq. (14) is

$$\frac{\partial \chi}{\partial \bar{p}} = a_{11} + 2a_{12}\bar{p} + 3a_7\bar{p}^2, \quad (24)$$

and Eq. (9) produces

$$\frac{d\bar{p}}{dx} = \frac{1}{B_w} \frac{dp(r, z)}{dx}. \quad (25)$$

By substituting $\sin \theta = z/r$, the pressure distribution in Eq. (4) can be restated as

$$p(r, t) = \frac{2Tp_o}{akz} e^{-\alpha'v^2r} e^{i(kr-\omega t)} J_1(ak \sin \theta). \quad (26)$$

Evaluation of Eq. (25) produces

$$\begin{aligned} & \frac{d\bar{p}(r, \theta, t)}{dx} \\ &= \frac{2Tp_o \Delta x}{B_w akzr} e^{-\alpha'v^2r} e^{i(kr-\omega t)} J_1(ak \sin \theta) \\ & \times \left[ik - \alpha v^2 - \frac{akz}{r^2} \frac{(J_0(ak \sin \theta) - J_2(ak \sin \theta))}{J_1(ak \sin \theta)} \right], \end{aligned} \quad (27)$$

where the relations $dr/dx = \Delta x/r$ and $d(\sin \theta)/dx = -\Delta xz/r^3$ have been used.

The physically observable pressure field is determined by substituting $-\phi = \omega t$ and taking the absolute value.

The calculation assumes that the laser acts as a single ray such that it is deflected as a single unit [22]. The validity of this assumption depends on the acoustic wavelength and the physical size of the beam. Significant departures from this will decrease the temporal resolution and diminish the ability to obtain higher frequency sensitivity.

3. Deflection as a Function of Frequency

After substitution, Eq. (21) was evaluated using quadrature integration for frequencies ranging from 2 kHz to 21 MHz. The temperature of water was set at 14°C, producing an ultrasound velocity of 1461 m/s. The initial pressure was set at $p_o = 1000$ Pa and the transducer radius at $a = 0.75$ cm. The integration is performed along the optical path z from -10 to 10 cm.

The results, shown in Fig. 4, possess a broadband response for positions $x = 2, 5,$ and 10 cm. Maximum sensitivity is reached between 1.4 and 1.9 MHz, with deflections that range from 0.42×10^{-3} to 0.49×10^{-3} degrees.

To allow easy comparison to hydrophones and transducers, the data are replotted in Fig. 5 with signal levels specified in decibels, according to the formula

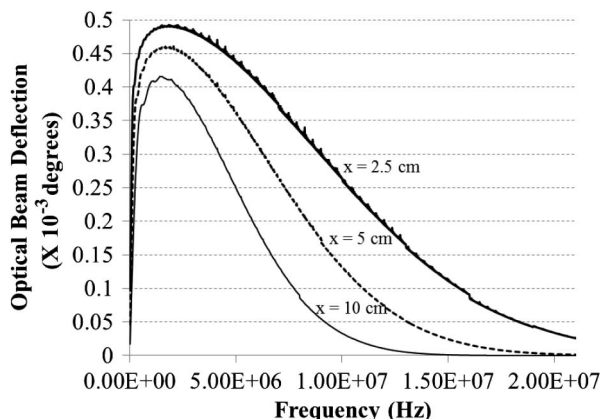


Fig. 4. Optical beam deflection as a function of frequency is shown for three distances. The plots demonstrate the reduction in signal at higher frequencies and that this technique has a broadband frequency response. Maximum sensitivity is achieved in the range of 1.4–1.9 MHz.

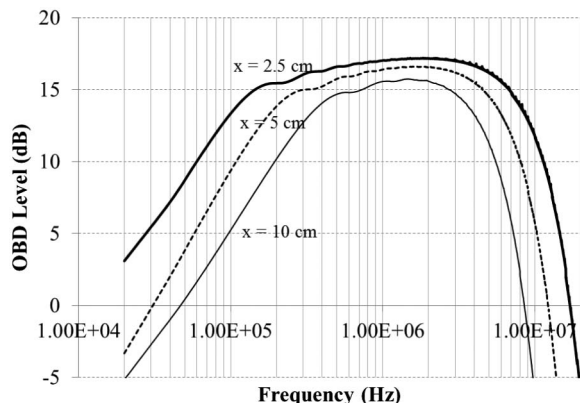


Fig. 5. Optical beam deflection level (displayed in decibels in reference to the minimal detectable deflection) as a function of frequency is shown for three distances. Values above 0 reflect frequencies that can be detected with state-of-the-art position-sensitive photodetectors.

$$\text{OBD}_{\text{dB}} = 20 \log_{10} \left(\frac{\theta_b}{\theta_{b \text{ min}}} \right), \quad (28)$$

where $\theta_{b \text{ min}}$ is an empirically derived minimal beam deflection angle as described in the next section.

The broadband nature of the signal is very apparent. For the case of $x = 2.5$ cm, the sensitivity stays within 10 decibels of the maximum signal from 40 kHz to 14.2 MHz. For $x = 5$ cm, this range extends from 50 kHz to 10 MHz. For $x = 10$ cm, the response still remains broad, extending from 105 kHz to 7.0 MHz.

4. Detection Sensitivity

The ability of the photodetector to sense lateral movements of the beam depends primarily on the sensitivity of the photocells and the laser power. In a previous paper [1], we demonstrated that the technique was capable of sensing lateral movements of less than $0.3 \mu\text{m}$ in air with the detector. This is consistent with other published results [23,24] and commercial products [25]. If the optical lever arm has a length $z = 0.25$ m, the minimum detectable beam deflection is $68 \mu\text{deg}$. A comparison of this value to the results displayed in Fig. 5 reveals that one can obtain detectable signals in the range of 15.8 kHz–13.6 MHz for $x = 10$ cm and 6.8 kHz to 14.1 MHz for $x = 5$ cm. An additional calculation performed for $x = 2.5$ cm revealed a detectable range from 100 Hz to 20.0 MHz, provided the original assumption regarding the beam size can be accommodated.

For a given frequency, the minimal detectable pressure can also be derived. With the frequency held constant at $\nu = 100$ kHz, Eq. (21) was evaluated for a range of pressures at our three values of x . As shown in Fig. 6, there is a linear relationship between the acoustic pressure and the optical beam deflection. The slope of the line allows the conversion from the minimal detectable beam deflection angle to the minimal detectable acoustic pressure for that frequency.

This calculation was repeated for 10 kHz, 1 MHz, and 10 MHz. The slopes derived are shown in Table 3 in units of microdegrees per pascal.

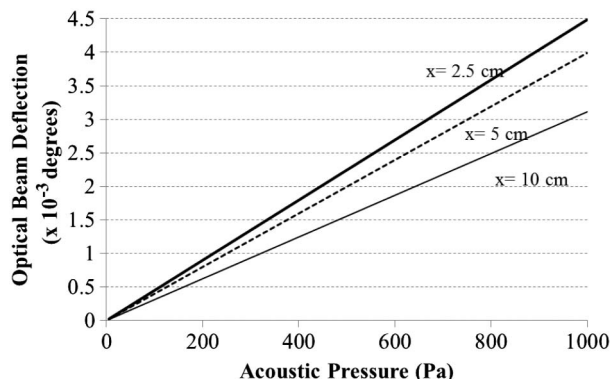


Fig. 6. Optical beam deflection level at 100 kHz as a function of acoustic pressure is shown for three distances. The calculation shows a linear relationship at all three distances.

Table 3. θ_b/p_o Columns are Conversion Factors Derived by Calculating the Slopes of Optical Beam Deflection as Functions of Acoustic Pressure^a

x (cm)	θ_b/p_o			p_{\min} (Pa)		
	2.5	5	10	2.5	5	10
10 kHz	1.183	0.690	0.399	57.5	98.6	170.4
100 kHz	4.487	3.991	3.112	15.16	17.04	21.85
1 MHz	5.068	4.907	4.690	13.42	13.86	14.50
10 MHz	2.617	1.324	0.343	25.99	51.36	198.05

^aThe slope values are in units of microdegrees per pascal. The p_{\min} columns give the minimal detectable acoustic pressure provided the minimal detectable beam deflection is 68 μ deg.

The minimal detectable acoustic pressures are shown in the last three columns in Table 3. It is interesting to note that when $\nu = 1$ MHz, the minimum is lower than at the other frequencies. We suspect that at lower pressures, the terms in Eq. (21) that depend on the first derivative of the pressure become more prominent than those dependent on the pressure.

5. Comments

In this paper, we have derived the frequency response of optical beam deflection as a result of an acoustic wave created by a piston in a liquid medium. The system exhibits broadband sensitivity from tens of kilohertz to near 10 MHz. The minimal detectable acoustic pressure was determined for various situations based on a minimal detectable lateral change. As such, the technique can be beneficial to a variety of areas.

For nondestructive evaluation, the technique can be used to complement or replace conventional immersion ultrasound transducers. An optical beam has an advantage over a transducer in that it does not interfere with the direction or the amplitude of the acoustic wave. Thus, a beam can sense the acoustic wave before and after the waveform interrogates the target, thus giving a more accurate waveform that is not distorted by the narrow frequency band of the transducer. In addition, the technique can be used in environments that would otherwise corrode the transducers.

The technique could also be used as a broadband directional sensor for maritime acoustic waves. Recent research demonstrated that the dependence on angle is strong [11]. With two beams and with the use of quad-cell directions, the direction of the source can be determined in three dimensions. This method could also find use in the calibration of conventional hydrophones.

References and Notes

1. J. N. Caron, "Displacement and deflection of an optical beam by airborne ultrasound," in *Review of Progress in Quantitative Nondestructive Evaluation*, D. O. Thompson and D. E. Chimenti, eds. (AIP, 2008), Vol. 975, pp. 247–254.
2. J. N. Caron, J. B. Mehl, and K. V. Steiner, "Gas-coupled laser acoustic detection," U.S. patent 6,041,020 (21 March 2000).

3. J. N. Caron, Y. Yang, J. B. Mehl, and K. V. Steiner, "Gas-coupled laser acoustic detection at ultrasonic and audio frequencies," *Rev. Sci. Instrum.* **69**, 2912–2917 (1998).
4. J. N. Caron, K. V. Steiner, Y. Yang, and J. B. Mehl, "Gas coupled laser acoustic detection for ultrasound inspection of composite materials," *Mater. Eval.* **58**, 667–671 (2000).
5. J. Diaci, "Transfer function of the laser beam deflection probe for detection of cylindrical acoustic waves in a transverse arrangement," *J. Phys. IV* **4**, C7-773–C7-776 (1994).
6. T. Matsuoka, A. Kumata, S. Koda, and H. Nomura, "Ultrasonic velocity measurement using optical beam deflection," *Jpn. J. Appl. Phys.* **34**, 2778–2780 (1995).
7. P.-K. Choi, "Broadband measurements of ultrasonic waves using optical beam deflection," in *AIP Conference Proceedings* (AIP, 2000), Vol. 524, pp. 325–328.
8. K. Yamaguchi and P.-K. Choi, "Probing focused sound fields using optical-beam deflection method," *Jpn. J. Appl. Phys.* **45**, 4621–4624 (2006).
9. R. Petkovšek and J. Možina, "Optodynamic characterization of shock waves after laser-induced breakdown in water," *Opt. Express* **13**, 4107–4112 (2005).
10. P. Gregorčič and J. Možina, "A beam-deflection probe as a method for optodynamic measurements of cavitation bubble oscillations," *Meas. Sci. Technol.* **18**, 2972–2978 (2007).
11. J. N. Caron and P. Kunapareddy, "Application of gas-coupled laser acoustic detection to gelatins and underwater sensing," in *40th Annual Review of Progress in Quantitative Nondestructive Evaluation* (AIP, 2014), Vol. 1581, pp. 458–463.
12. See, for example, "Waveform and defect detection" at NDT Resource Center at <http://www.ndt-ed.org>.
13. J. N. Caron, "Displacement and deflection sensitivity of gas-coupled laser acoustic detection," in *1st International Symposium on Laser Ultrasonics: Science, Technology and Applications*, 2008.
14. R. L. Whitman and A. Korpel, "Probing of acoustic surface perturbations by coherent light," *Appl. Opt.* **8**, 1567–1576 (1969).
15. L. Noui and R. J. Dewhurst, "A laser beam deflection technique for the quantitative detection of ultrasonic Lamb waves," *Ultrasonics* **31**, 425–432 (1993).
16. D. Royer, M.-H. Noroy, and M. Fink, "Optical generation and detection of elastic waves in solids," *J. Phys. IV* **4**, C7-673–C7-684 (1994).
17. P. M. Morse and K. U. Ingard, *Theoretical Acoustics* (McGraw-Hill, 1968).
18. C. S. Clay and H. Medwin, *Acoustical Oceanography* (Wiley, 1977).
19. R. Fernandez-Prini and R. B. Dooley, *The International Association for the Properties of Water, and Steam* (1998).
20. M. Born and E. Wolf, *Principles of Optics: Electromagnetic Theory of Propagation, Interference and Diffraction of Light* (Cambridge University, 1999).
21. J. N. Caron, "Application of laser ultrasonics to polymer/graphite composites," Ph.D. dissertation (University of Delaware, 1997).

22. G. P. Davidson and D. C. Emmony, "A schlieren probe method for the measurement of the refractive index profile of a shock wave in a fluid," *J. Phys. E* **13**, 92–97 (1980).
23. Z.-j. Gao, L.-l. Dong, and W.-h. Xu, "Design and analysis of displacement measurement system based on the four-quadrant detector," *Proc. SPIE* **8905**, 890531 (2013).
24. K. B. Fielhauer, B. G. Boone, J. R. Bruzzi, B. E. Kluga, J. R. Connelly, M. M. Bierbaum, J. J. Gorman, and N. G. Dagalakis, "Comparison of macro-tip/tilt and mesoscale position beam-steering transducers for free-space optical communications using a quadrant photodiode sensor," in *Optical Science and Technology, SPIE's 48th Annual Meeting* (International Society for Optics and Photonics, 2004), pp. 192–203.
25. See, for example, literature on the ThorLabs PDQ80A Segmented Quadrant Positioning Sensing Detector.